

Multicriteria Optimization of Lower Limb Exoskeleton Mechanism

Sayat Ibrayev

Professor
Joldasbekov Institute of
Mechanics and Engineering
Almaty, Kazakhstan, 050010
Email: sayat_m.ibrayev@mail.ru

Arman Ibrayeva*

Senior Research Scientist
Joldasbekov Institute of
Mechanics and Engineering
Almaty, Kazakhstan, 050010
Email: arman.ibrayeva@kaust.edu.sa

Ayaulym Rakhmatullina

Associate Professor
Department of Engineering Graphics
and Applied Mechanics
Almaty Technological University
Almaty, Kazakhstan, 050012

Aizhan Ibrayeva

Scientist
Megalabs, Palo Alto, CA 94301

Bekzat Amanov

Senior Research Scientist
Joldasbekov Institute of
Mechanics and Engineering
Almaty, Kazakhstan, 050010

Nurbibi Imanbayeva

Associate Professor
Department of Mechanical Engineering
Satbayev University
Almaty, Kazakhstan, 050000

ABSTRACT

Typical leg exoskeletons employ open-loop kinematic chains with motors placed directly on movable joints; while this design offers flexibility, it leads to increased costs and heightened control complexity due to the high number of degrees of freedom. The use of heavy servo-motors to handle torque in active joints results in complex and bulky designs, as highlighted in existing literature. In this study, we introduced a novel synthesis method with analytical solutions provided for synthesizing lower-limb exoskeleton. Additionally, we have incorporated multicriteria optimization by six designing criteria. As a result, we offer several mechanisms, comprising only six links, well-suited to the human anatomical structure, exhibit superior trajectory accuracy, efficient force transmission, satisfactory step height, and having internal transfer segment of the foot.

1 Introduction

Exoskeleton robots have found broad application for augmenting power and aiding in rehabilitation [1, 2, 3, 4, 5, 6, 11]. Power augmentation is important for tasks involving heavy load transportation with limited muscle strength, while robot-assisted technologies employing upper and lower limb exoskeletons are used for rehabilitating individuals who have experienced a loss of mobility in their joints and muscles. Studying human walking apparatus and motion diagrams representing the leg movement were useful in various fields including the development of human prosthetics, human mimicking robots, and advancements in research areas such as biomimetics, military combat, cinematography, toys, and terrestrial and extraterrestrial exploration [11, 24]. For a comprehensive overview of bipedal walking robots and exoskeletons, refer to [1, 2, 3, 4].

Various design and control architectures of exoskeletons were summarized in the relevant references [5, 3]. In recent years, various design schemes of lower limb exoskeletons aimed at achieving compact devices and meeting specific optimality criteria have been proposed [25, 12, 30]. Commonly, the kinematic scheme of the leg exoskeleton is based on an

*Corresponding author

open-loop kinematic chain with the motors mounted directly on the movable joints. While these open kinematic chains offer greater flexibility and ease of design, their large number of degrees of freedom (DOF) contributes to increased costs and complexities in control. Using heavy servo-motors to meet significant torques generated in active joints leads to complicated and cumbersome design. The bulkiness and substantial weight of this kind of devices are highlighted in [6, 7].

Numerous researchers have studied the walking apparatus, demonstrating that walking patterns are measurable, predictable, and repeatable. [9] presents a passive exoskeleton with 17 DOF for load-carrying, which includes two 3 DOF ankle joints, two 2 DOF hip joints, two 1 DOF knee joints, a 1 DOF backpack, and two redundant degrees of freedom at the thigh and the shank to improve the compatibility of human-machine locomotion. In [8], a mechanism has been designed for a walking robot, effectively minimizing the number of required motors, thereby contributing to reduced energy consumption. The dimensional synthesis is conducted analytically to formulate a parametric equation, and the resulting geometry of the leg mechanism is established. However, it should be noted that this mechanism is not suitable for exoskeletons due to its significant deviation in shape from that of the human leg.

Shen et al. [7,6] introduced a 1 DOF mechanism for lower limb rehabilitation exoskeletons. In [7] proposed an integrated type and dimensional synthesis method for designing compact 1 DOF planar linkages with only revolute joints, and applied the method on a leg exoskeleton that can generate human gait patterns simultaneously at hip and knee joints. Reducing the number of motors resulted in decreased energy consumption. [6] reports a close match to human gait and stable hip and knee joint outputs in their prototype due to its parallel structure. The drawback of Shen's mechanism is its use of an 8-bar-10-joint configuration, simplification would involve reducing the number of these linkages.

[10] presents a leg exoskeleton consisting of a planar five links closed linkage. The robotic system is intended for patients who have suffered strokes. The design is simple, wearable and light, with anthropomorphic structure, and operates with only one motor. The drawbacks mentioned in the paper include the limitation of providing mobility solely to the knee and hip joints, as well as the need for future design improvements, such as an adjustable length mechanism to accommodate patients with varying anthropometric data. In [12] the author introduced a new 1 DOF structure allowing adjustments of mechanism links to accommodate varying human body types. However, the geometry of the novel design is bulkier. The exoskeleton is based on seven-link mechanism, is cost-effective and easy to implement in practical activities. This leg mechanism can assure the mobility of knee and hip joints, and the ankle joint was not considered in favor of reducing the cost. Also the paper states that its design may require additional improvements in future developments, such as the foot shape optimization. Another study [11] focuses on the experimental and numerical study of human gait. Its results have practical applications in the design and development of human-inspired robotic structures for use in medical, assistive, or rehabilitation fields. Specifically, the study aims to investigate the flexion-extension movements of lower limb joints in humans and analyze the ground reaction forces generated during walking on force platforms.

Plecnik proposed a synthesis method for six-bar mechanisms [26], which was applied to explore one million tasks, resulting in the synthesis of one hundred and twenty two practical linkage designs. In [27] the author presents a design procedure for Stephenson I-III six-bar linkages that is demonstrated on the design of legs. These mechanisms are advantageous for their simplicity, characterized by a reduced number of links. While suitable for applications such as walking robots, they may not meet the requirements for exoskeletons, which demand designs that closely conform to the human anatomy while emphasizing compactness. Hence, the quest for more compact solutions in the context of exoskeletons continues.

Demonstration of a 1 DOF closed-loop mechanical linkage that can be designed to the shape and movement of a biped human walking apparatus is presented also in [13]. A single DOF eight-bar path generator that typifies the shape and motion of a human leg is proposed. However, the relative foot stride is notably small. This concept was developed by the authors in [14] towards minimizing the number of links, and a six-link leg mechanism for a biped robot was synthesized. Unfortunately, they used prismatic joints, and the foot stride is small as well. An eight-bar walking mechanism was designed in [15], but the foot path does not have a straight-line segment that will correspond to the support phase (when the foot contacts the ground).

Design and optimization of a 1 DOF eight-bar leg mechanism for a walking machine was proposed in [16]. The leg mechanism is considered to be very energy efficient, especially when walking on rough terrains. Furthermore, the mechanism requires very simple controls since a single actuator is required to drive the leg. Dynamic analysis was performed to evaluate the joint forces and crank torques of each solution, thus taking into account inertia forces in the design. Two critical aspects of the leg mechanism's performance were chosen to be optimized: minimizing the energy to improve the efficiency of the leg and lowering the requirement for larger motors, and second, maximizing the stride length because a leg that travels a longer distance with lower energy is very desirable. Hence, the energy per unit of travel was reduced. However, the total design obtained was cumbersome, since the mechanism was based on Theo Jansen's straight-line generator.

The synthesis of leg mechanisms inspired from Theo-Jansen's solution has been a research topic in the last years [17, 18] for its advantages regarding the reduced number of DOFs which makes it easier to control, the scalable design, the reduced impact on the ground during walking, and because of less energy consumption. The Theo-Jansen mechanism was developed in [17] considering an adaptive and controllable mechanism on irregular ground. This research sets a basis for further extension of the Theo-Jansen mechanism, considering the bending of the leg linkages while turning and providing high stiffness of design. The prototype developed was tested at various speeds and torques due to presence of the speed control

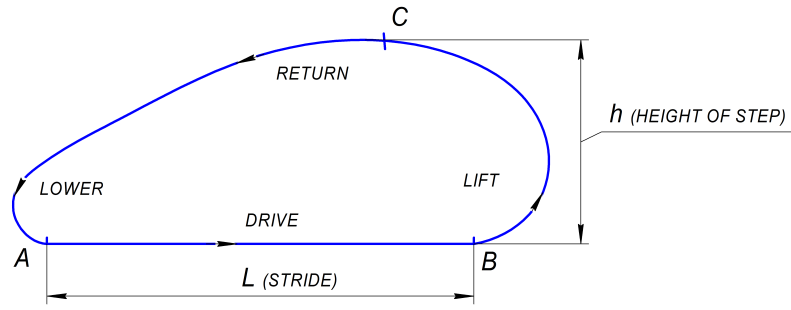


Fig. 1: Prof. J. Shigley's Foot-Path Diagram

system provided in electronic system, which enables to use the prototype for various load handling capacities. An eight-bar leg mechanism dimensional synthesis is presented in [18] as well. As compared to the prototype, the advantage of the proposed geometric model consists of a greater step height that helps the robotic structure to overcome larger obstacles.

The Klann linkage is another single DOF walking mechanism that is patented and is widely used on multi-legged robots [19, 20, 21, 22]. The capabilities of standard non-reconfigurable quadruped Klann legs can be significantly extended applying the method proposed in [19]. Reconfigurable legged robots based on 1 DOF Klann mechanism are highly desired because they are effective on rough and irregular terrains and they provide mobility in such terrain with simple control schemes. However, both Theo Jansen's solution and Klann mechanism inspired leg designs are very cumbersome, especially they cannot be used as lower limb exoskeleton since it does not fit the size limit and overall dimension restrictions. Other related works include [29, 31, 35, 36, 37, 38].

Tsuge [23] proposed a kinematic synthesis method developed to achieve a mechanical system that guides a natural ankle trajectory for human walking gait. The author analyzed existing Watt I and Stephenson III six-bar linkage synthesis methods and applied the developed additional linkage synthesis procedures for treadmill training mechanism design. A new six-bar linkage system was proposed to support natural movement of the human lower limb. However the accuracy of generated straight-line segment of foot path is poor and relative horizontal velocity of the foot is not constant.

In [28] presented 6 configurations of an 8-bar leg mechanism, with three fixed pivots that make it strong and stable, validated on experimental prototype. The paper emphasizes that this mechanism offers the largest stride-to-size ratio, allowing for the construction of a compact and lightweight walking mechanism with low inertia. Consequently, it is well-suited for speed walking. In this study we synthesized a mechanism that is even more compact, and comprising only six links. We introduced a novel synthesis method, and as the result of multicriteria optimization, we achieved a compact solution matching human anatomy, with high accuracy of trajectory generation, optimized force transfer, minimized chassis height, and with internal transfer of foot.

The desired foot trajectory consists of two segments (Fig. 1):

1. straight-line segment $A - B$ with stride L , corresponding to the *support phase* of step cycle (when the foot P is on the ground);
2. swing phase segment $B - C - A$ with a step height h (the *leg transfer phase*).

This paper is organized as follows: Section 2 introduces the structure of the lower-limb exoskeleton mechanism and our proposed synthesis method. Section 3 presents analytical solutions of the synthesis problem. Multicriteria optimization conditions are defined in Section 4. Obtained design solutions are discussed in Section 5, and the final design is presented in Section 6. And Section 7 provides conclusions.

2 Lower Limb Exoskeleton Mechanism Structure and Synthesis Problem Formulation

Human walking can be analyzed in three planes: the sagittal plane, coronal plane, and transverse plane [6, 7]. Among these, the sagittal plane motion is predominant. The designed leg exoskeleton aids in hip and knee flexion/extension movements while the wearer stays in place. This practice focuses on motions within the sagittal plane. Consequently, a planar linkage with angular outputs can effectively facilitate these movements.

The kinematic scheme of six-bar Stephenson III type lower-limb exoskeleton mechanism is illustrated in Fig. 2a with the input link AB and the foot P mounted on coupler EF . Rotation of the crank AB is described by φ_i ,

$$\varphi_i = \varphi_0 + \Delta\Phi \frac{i-1}{N-1}, \quad i = \overline{1, N}. \quad (1)$$

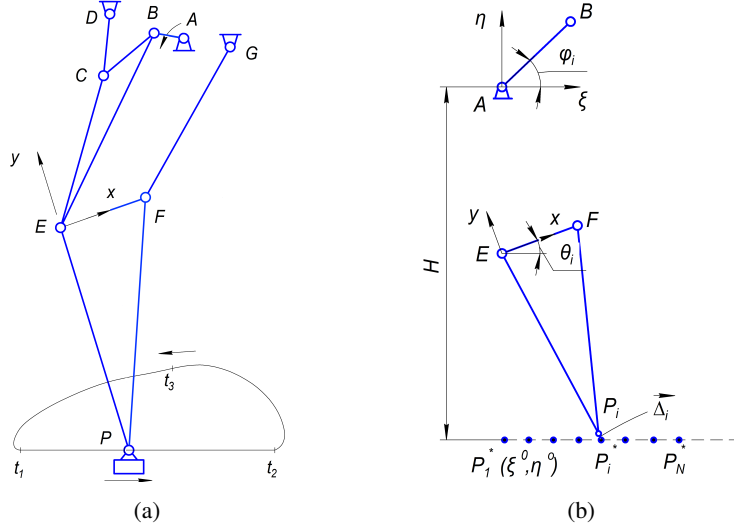


Fig. 2: Kinematic scheme of a lower-limb exoskeleton mechanism

Here, φ_0 is an initial angular position of the crank AB with respect to the horizontal axis. $\Delta\Phi$ is the maximum rotation angle, $\Delta\Phi > \pi$, in order to supply the overlap of support phases of alternating two legs. **Kinematic analysis** of the mechanism is provided in Appendix A.

The rotation of the crank GF is represented by the angle θ_i , $i = \overline{1, N}$. $\vec{r}_P[x_P, y_P]$ is a local radius vector, rigidly associated with the moving coordinate system Exy ; and $\vec{R}_{P_i}[\xi_{P_i}, \eta_{P_i}]$ and $\vec{R}_{E_i}[\xi_{E_i}, \eta_{E_i}]$ signify the absolute positions of the foot center P_i and the point E respectively. Then the relationship for \vec{R}_{P_i} can be expressed as:

$$\vec{R}_{P_i} = \vec{R}_{E_i} + \Gamma(\theta_i)\vec{r}_P = \begin{bmatrix} \xi_{E_i} \\ \eta_{E_i} \end{bmatrix} + \begin{bmatrix} x_P \cos \theta_i - y_P \sin \theta_i \\ x_P \sin \theta_i + y_P \cos \theta_i \end{bmatrix}, \quad (2)$$

Given the desired absolute coordinates of the foot P_i^* (Fig. 2b):

$$\xi_{P_i^*} = \xi^0 + L \frac{i-1}{N-1}, i = \overline{1, N}$$

$$\eta_{P_i^*} = \eta^0,$$

with stride L and desired start position $P_1^*(\xi^0, \eta^0)$, the synthesis condition is stated as follows:

$$\vec{\Delta}_i \equiv \vec{R}_{P_i} - \vec{R}_{P_i^*} = \vec{0}, \quad i = \overline{1, N}. \quad (3)$$

Considering the constraint equations Eq. (2) one can write in scalar form as follows:

$$\begin{aligned} \delta_i^\xi &= x_P \cos \theta_i - y_P \sin \theta_i - \xi^0 + \xi_{E_i} - L \frac{i-1}{N-1} = 0 \\ \delta_i^\eta &= x_P \sin \theta_i + y_P \cos \theta_i - \eta^0 + \eta_{E_i} = 0. \end{aligned} \quad (4)$$

Given the mechanism link lengths except (x_P, y_P) , synthesis task consists in determining the parameters $x_P, y_P, \xi^0, \eta^0, L$ that satisfy these constraints approximately.

Then the least square approximation problem is formulated as follows:

$$S = \sum_{i=1}^N \left((\delta_i^\xi)^2 + (\delta_i^\eta)^2 \right) \rightarrow \min_{\vec{x}}. \quad (5)$$

3 Analytical Solution of the Synthesis Problem

3.1 4-parameter synthesis

Unknown variables are:

$$x_1 := x_P, x_2 := y_P, x_3 := \xi^0, x_4 := \eta^0.$$

The conditions $\frac{\partial S}{\partial x_j} = 0, j = \overline{1, 4}$ lead to the following equations involving four unknowns x_1, x_2, x_3, x_4 :

$$\sum_{i=1}^N \left(\delta_i^\xi \cdot \frac{\partial \delta_i^\xi}{\partial x_j} + \delta_i^\eta \cdot \frac{\partial \delta_i^\eta}{\partial x_j} \right) = 0, \quad j = \overline{1, 4}. \quad (6)$$

Namely,

$$\sum_{i=1}^N \delta_i^\xi \cos \theta_i + \sum_{i=1}^N \delta_i^\eta \sin \theta_i = 0 \quad (7)$$

$$-\sum_{i=1}^N \delta_i^\xi \sin \theta_i + \sum_{i=1}^N \delta_i^\eta \cos \theta_i = 0 \quad (8)$$

$$\sum_{i=1}^N \delta_i^\xi = 0 \quad (9)$$

$$\sum_{i=1}^N \delta_i^\eta = 0 \quad (10)$$

Let us introduce notations:

$$k := \sum_{i=1}^N \cos \theta_i, \quad (11a)$$

$$m := \sum_{i=1}^N \sin \theta_i, \quad (11b)$$

$$b_1 := \sum_{i=1}^N \left(-\xi_{E_i} + L \cdot \frac{i-1}{N-1} \right) \cos \theta_i - \sum_{i=1}^N \eta_{E_i} \sin \theta_i, \quad (11c)$$

$$b_2 := \sum_{i=1}^N \left(\xi_{E_i} - L \cdot \frac{i-1}{N-1} \right) \sin \theta_i - \sum_{i=1}^N \eta_{E_i} \cos \theta_i, \quad (11d)$$

$$b_3 := \sum_{i=1}^N \left(-\xi_{E_i} + L \cdot \frac{i-1}{N-1} \right), \quad (11e)$$

$$b_4 := \sum_{i=1}^N (-\eta_{E_i}). \quad (11f)$$

Then we come to the system of linear equations expressed as follows:

$$Nx_1 - kx_3 - mx_4 = b_1 \quad (12a)$$

$$Nx_2 + mx_3 - kx_4 = b_2 \quad (12b)$$

$$kx_1 - mx_2 - Nx_3 = b_3 \quad (12c)$$

$$mx_1 + kx_2 - Nx_4 = b_4 \quad (12d)$$

The only solution of this system in case $k^2 + m^2 \neq N^2$ is

$$x_1 = \frac{-Nb_1 + kb_3 + mb_4}{k^2 + m^2 - N^2} \quad (13)$$

$$x_2 = \frac{-Nb_2 - mb_3 + kb_4}{k^2 + m^2 - N^2} \quad (14)$$

$$x_3 = \frac{Nb_3 - kb_1 + mb_2}{k^2 + m^2 - N^2} \quad (15)$$

$$x_4 = \frac{Nb_4 - mb_1 - kb_2}{k^2 + m^2 - N^2}. \quad (16)$$

The necessary conditions also serve as sufficient conditions for attaining the minimum of the function S : the matrix

$$\frac{d^2S}{d\vec{x}^2} = \begin{bmatrix} N & 0 & -k & -m \\ 0 & N & m & -k \\ -k & m & N & 0 \\ -m & -k & 0 & N \end{bmatrix}$$

is positive-definite (in case $k^2 + m^2 \neq N^2$), since the determinants of all corner minors are non-negative:

$$\begin{aligned} \Delta_1 &= N > 0, & \Delta_2 &= N^2 > 0, & \Delta_3 &= N^3 + N(k^2 + m^2) > 0, \\ \Delta_4 &= (k^2 + m^2 - N^2)^2 > 0. \end{aligned} \quad (17)$$

3.2 5-parameter synthesis

Let's explore a scenario where $L = x_5$ is an additional variable subject to optimization. Referring to Eq. (12), from the condition $\frac{\partial S}{\partial \vec{x}} = \vec{0}$ we get

$$Nx_1 - kx_3 - mx_4 - \sum_{i=1}^N \left(\frac{i-1}{N-1} \cos \theta_i \right) x_5 = b_5, \quad (18)$$

where

$$b_5 = \sum_{i=1}^N (-\xi_{P_i} \cdot \cos \theta_i - \eta_{P_i} \cdot \sin \theta_i)$$

$$Nx_2 + mx_3 - kx_4 + \sum_{i=1}^N \left(\frac{i-1}{N-1} \sin \theta_i \right) x_5 = b_6, \quad (19)$$

where

$$b_6 = \sum_{i=1}^N (\xi_{P_i} \cdot \sin \theta_i - \eta_{P_i} \cdot \cos \theta_i)$$

$$kx_1 - mx_2 - Nx_3 - \sum_{i=1}^N \left(\frac{i-1}{N-1} \right) x_5 = b_7, \quad (20)$$

where

$$b_7 = - \sum_{i=1}^N \xi_{P_i}$$

$$mx_1 + kx_2 - Nx_4 = b_8, \quad (21)$$

where

$$b_8 = - \sum_{i=1}^N \eta_{P_i} = b_4.$$

The last equation is derived from Eq. (6), $j = 5$:

$$\begin{aligned} & \sum \left(\frac{i-1}{N-1} \cos \theta_i \right) x_1 - \sum \left(\frac{i-1}{N-1} \sin \theta_i \right) x_2 \\ & - \sum \left(\frac{i-1}{N-1} \right) x_3 + \sum \left(\frac{i-1}{N-1} \xi_{P_i} \right) x_4 + \sum \left(\frac{i-1}{N-1} \right)^2 x_5 = 0. \end{aligned} \quad (22)$$

Finally, taking into account

$$\sum \left(\frac{i-1}{N-1} \right) = N/2 \quad (23)$$

and

$$\sum \left(\frac{i-1}{N-1} \right)^2 = \frac{N(2N-1)}{6(N-1)}, \quad (24)$$

we obtain the following system of linear equations

$$A\vec{x} = \vec{b}, \quad (25)$$

where

$$A = \begin{bmatrix} N & 0 & -k & -m & -k_\alpha \\ 0 & N & m & -k & k_\beta \\ k & -m & -N & 0 & -N/2 \\ m & k & 0 & -N & 0 \\ k_\alpha & -k_\beta & -N/2 & 0 & -\frac{N(2N-1)}{6(N-1)} \end{bmatrix} \quad (26)$$

$$\vec{b} = [b_5 \ b_6 \ b_7 \ b_8 \ -k_\mu]^T \quad (27)$$

and

$$k_\alpha := \sum \left(\frac{i-1}{N-1} \cos \theta_i \right) \quad (28)$$

$$k_\beta := \sum \left(\frac{i-1}{N-1} \sin \theta_i \right) \quad (29)$$

$$k_\mu := \sum \left(\frac{i-1}{N-1} \xi_{P_i} \right) \quad (30)$$

The Hessian $H_S = \frac{d^2 S}{dx^2}$, and it is non-negative definite (for the proof refer to Appendix B).

$$H_S = \begin{bmatrix} N & 0 & -k & -m & -k_\alpha \\ 0 & N & m & -k & k_\beta \\ -k & m & N & 0 & N/2 \\ -m & -k & 0 & N & 0 \\ -k_\alpha & k_\beta & N/2 & 0 & \frac{N(2N-1)}{6(N-1)} \end{bmatrix},$$

Therefore, the last condition supplies the minimum of the function S , if $\det H_S \neq 0$. For analytical solution in this case we refer to Eq. (12a) – (12d):

$$x_1 = \frac{b_5 + kx_3 + mx_4 + k_\alpha x_5}{N} \quad (31)$$

$$x_2 = \frac{b_6 - mx_3 kx_4 - k_\beta x_5}{N} \quad (32)$$

$$x_3 = \frac{Nb_7 + \frac{N^2}{2}x_5 - kb_5 - kk_\alpha x_5 + mb_6 - mk_\beta x_5}{k^2 + m^2 - N^2} \quad (33)$$

$$x_4 = \frac{Nb_8 - mb_5 - mk_\alpha x_5 - kb_6 + kk_\beta x_5}{k^2 + m^2 - N^2}, \quad (34)$$

assuming $k^2 + m^2 \neq N^2$; and x_5 can be found directly by substituting Eq. (31) – (34) into Eq. (22).

4 Additional Synthesis Conditions and Multiple Optimization Criteria

In order to choose the acceptable solutions from a trial table, which contains great amount of data, a certain design criteria will be used. The trajectory of the foot center P , called a step cycle, consists of two phases: “support phase” and “transfer phase” (swing). During the support phase the foot center P should trace horizontal straight-line. The *main criteria* of synthesis is the accuracy of straight line generation during support phase, that has to be minimized:

$$c_1 = \max_{i=1, N} |\eta_P^0 - \eta_{P_i}|. \quad (35)$$

At the same time we deal with a complicated synthesis task since the following additional criteria should be taken into account.

The chassis height $H = -x_4$ has to be minimized or (which is the same condition) $\eta^0 = -H$ to be maximized:

$$c_2 = x_4 \quad (36)$$

The worse transference angle has to be maximized

$$c_3 = \min_{0 \leq \varphi \leq 2\pi} (\mu_{BCD}, \mu_{EFG}) \quad (37)$$

where

$$\begin{aligned} \mu_{BCD} &= \arccos \frac{L_{BC}^2 + L_{CD}^2 - |BD|^2}{2L_{BC}L_{CD}}, \\ \mu_{EFG} &= \arccos \frac{L_{EF}^2 + L_{FG}^2 - |EG|^2}{2L_{EF}L_{FG}}, \end{aligned} \quad (38)$$

$L_{BC}, L_{CD}, L_{FG}, L_{EF}$ are lengths of corresponding links, $|BD|, |EG|$ are distances between the centers of corresponding joints.

Anatomy matching: hip to shin relation L_{FP}/L_{FG} (the ratio of the thigh to the lower leg) has to be around one ($c_4 = 1$)

$$c_4 = L_{FP}/L_{FG} \quad (39)$$

The penalty function c_5 for external transfer of the foot center P has to be minimized.

$$c_5 = \sum_{i=1}^N \max((\eta^0 - \eta_{P_i}), 0) \quad (40)$$

If $\eta_{P_i} < \eta^0$, then the penalty function c_5 will be increased to positive value $\max((\eta^0 - \eta_{P_i}), 0)$. Otherwise, if $\eta_{P_i} \leq \eta^0$, then $\max((\eta^0 - \eta_{P_i}), 0) = 0$, thus nothing will be added to the function c_5 .

5 Global Search and Multi-Criteria Optimization of Exoskeleton Link Dimensions

Let us keep notation ξ, η for absolute coordinates of joints as it was in the previous sections.

$n = 13$ variable parameters of the exoskeleton mechanism are varied within a given search area by using so called random LP- τ sequences, evenly distributed in n -dimensional parallelepiped [32, 33, 34]. Global search carried out specifying the following limits on variable parameters

$$\begin{aligned}
-1.50 &\leq \eta_D \leq 1.50 \\
-1.50 &\leq \xi_G \leq 1.50 \\
-1.50 &\leq \eta_G \leq 1.50 \\
0.05 &\leq r_{AB} \leq 0.30 \\
0^\circ &\leq \phi_0 \leq 360^\circ \\
180^\circ &\leq \Phi \leq 190^\circ \\
0.40 &\leq L_{BC} \leq 1.00 \\
0.40 &\leq L_{CD} \leq 1.00 \\
0.50 &\leq x_E \leq 1.20 \\
-0.50 &\leq y_E \leq 1.20 \\
0.10 &\leq L_{EF} \leq 0.40 \\
0.30 &\leq L_{FG} \leq 1.10,
\end{aligned}$$

where

- $\xi_D, \eta_D, \xi_G, \eta_G$ are the absolute coordinates of frame joints D and G ;

- r_{AB} is the length of crank AB ;

- x_E, y_E are the local coordinates of joint E relative to the Bx_2y_2 moving coordinate system, with the Bx_2 axis along line BC ; The foot-point traces a straight line while the crank angle is in the range $\phi_0 \leq \phi \leq \phi_0 + \Delta\Phi$.

The notation p_1, p_2, \dots, p_{13} is used in the tables for these parameters: $p_1 := \xi_D, p_2 := \eta_D, p_3 := \xi_G, p_4 := \eta_G, p_5 := r_{AB}, p_6 := \phi_0, p_7 := \Phi, p_8 := L_{BC}, p_9 := L_{CD}, p_{10} := x_E, p_{11} := y_E, p_{12} := L_{EF}, p_{13} := L_{FG}$.

For each set of $n = 13$ random variables analytical solutions for 5 design parameters x_1, x_2, \dots, x_5 are determined applying formulae Eq. (31) – (34), and Eq. (22), and the trial table is obtained by calculating design criteria values. Analyzing the obtained trial table, 25 preliminary solutions are selected as specified in Table 1 and shown in Fig. 7 (7). The criteria values (c_1, \dots, c_5) for the obtained solutions are found to be vary within the following limits:

$$\begin{aligned}
0 \leq c_1 \leq 0.05; \quad -1.6 \leq c_2 \leq -0.70; \quad 27 \leq c_3 \leq 90; \\
0.5 \leq c_4 \leq 2.0; \quad 0 \leq c_5 \leq 15.00
\end{aligned} \tag{41}$$

The parameter values for solution on Fig. 7a are shown in Tables 11-13 (Appendix C)

Global Search within the Narrowed Search Area. Analyzing the results, we study functionality of the mechanism. The most elusive was meeting criteria c_5 (achieving internal swing with trajectory turned inward). Thus, a design criterion c_6 was introduced to increase the step height $h_i = \eta_{P_i} - \eta^0$ defined as

$$c_6 = \sum_{i=1}^N h_i, \tag{42}$$

that has to be maximized. (Note that we have not used $h = \max h_i$ as a design criterion c_6 , since it does not reflect the foot trajectory that goes below the limit $\eta = \eta^0$ as demonstrated in Fig. 7 (Appendix C). Meanwhile, when using the sum these trajectories will have negative sign which decreases the sum). Arranging and cutting the obtained trial table, eliminating solutions with unacceptable criteria values, we are looking for the compromise solutions that meet all designing criteria, so we clarify new boundaries for design variables. Then we carry out new search of the design parameters within the new search area and obtain new trial table. After several repetition of this sequence of actions we came to the following search area specified by the boundaries:

Table 1: Trial table fragment: criteria values with the limits specified by Eq. (41)

| LPτ № | Fig | c_1 | c_2 | c_3 | c_4 | c_5 |
|-------|-----|---------|-----------|-----------|---------|-----------|
| 19597 | 7a | 0,01248 | -147,377 | 3,624,502 | 0,72546 | 0,81125 |
| 20108 | 7b | 0,01147 | -158,420 | 5,885,124 | 108,176 | 416,844 |
| 4327 | 7c | 0,01502 | -137,035 | 3,793,790 | 0,83849 | 0,73034 |
| 23379 | 7d | 0,01254 | -150,056 | 3,116,345 | 0,79369 | 114,581 |
| 16038 | 7e | 0,01413 | -156,780 | 4,855,631 | 0,70010 | 225,781 |
| 17217 | 7f | 0,01566 | -158,656 | 4,388,126 | 0,49570 | 0,98881 |
| 15985 | 7j | 0,01930 | -146,579 | 3,042,169 | 0,98595 | 246,731 |
| 18709 | 7h | 0,02863 | -152,807 | 3,897,082 | 0,51939 | 114,727 |
| 25950 | 7i | 0,02381 | -129,038 | 5,426,018 | 162,689 | 818,859 |
| 12502 | 7j | 0,02398 | -147,632 | 3,400,994 | 0,63502 | 653,650 |
| 12709 | 7k | 0,03239 | -139,157 | 2,736,399 | 117,269 | 833,609 |
| 4149 | 7l | 0,03486 | -130,577 | 4,095,673 | 115,044 | 904,692 |
| 7934 | | 0,01531 | -137,623 | 2,599,608 | 102,889 | 263,405 |
| 25906 | | 0,01791 | -148,873 | 5,359,325 | 197,100 | 608,409 |
| 26153 | | 0,01821 | -145,573 | 3,598,747 | 0,85130 | 368,757 |
| 16074 | | 0,02117 | -157,979 | 3,669,121 | 0,76626 | 317,949 |
| 4838 | | 0,02171 | -1,321063 | 3,955,225 | 0,99599 | 694,072 |
| 29001 | | 0,02532 | -131,698 | 2,974,295 | 168,845 | 350,371 |
| 11761 | | 0,02588 | -151,677 | 3,248,405 | 0,68656 | 113,792 |
| 379 | | 0,02937 | -111,082 | 2,736,639 | 185,211 | 455,336 |
| 12658 | | 0,02942 | -155,801 | 4,313,619 | 167,947 | 789,940 |
| 15834 | | 0,03027 | -146,200 | 5,063,574 | 160,647 | 689,696 |
| 7260 | | 0,03258 | -131,509 | 4,130,343 | 192,072 | 1,026,527 |
| 32037 | | 0,03713 | -144,800 | 3,883,024 | 124,053 | 838,340 |

$$-0.77 \leq \xi_D \leq -0.05$$

$$-0.84 \leq \eta_D \leq 0.05$$

$$-0.95 \leq \xi_G \leq -0.06$$

$$-0.91 \leq \eta_G \leq 0.04$$

$$0.07 \leq r_{AB} \leq 0.22$$

$$-110^\circ \leq \varphi_0 \leq -9^\circ$$

$$180^\circ \leq \Phi \leq 190^\circ$$

$$0.20 \leq L_{BC} \leq 0.75$$

$$0.19 \leq L_{CD} \leq 0.60$$

$$0.80 \leq x_E \leq 2.22$$

$$-0.70 \leq y_E \leq 1.07$$

$$0.17 \leq L_{EF} \leq 0.62$$

$$0.57 \leq L_{FG} \leq 1.91.$$

As the result we obtained a number of solutions presented on Table 2, having internal transfer segment of the foot, so that in the swing phase the foot trajectory is turned inward. Part of these solutions are plotted on Fig. 3. The solutions in Table 2 are arranged by criterion c_6 in descending order. Despite the step height (height of the foot transference) not being very high, we obtained the desired solutions with high accuracy (about 1 percent from step stride) and fine transmission angle (from 32° to 55°) (Tables 3 – 5).

Table 2: The trial table fragment: the best solutions by criterion c_6

| LPt № | Fig. | c_1 | c_2 | c_3 | c_4 | c_5 | c_6 |
|-------|------|--------------|---------------|-------------|--------------|-------|-------|
| 29884 | 3a | 0,011 | -2,028 | 32,8 | 0,351 | 0,332 | 5,504 |
| 31076 | 3b | 0,011 | -2,411 | 54,8 | 0,865 | 0,329 | 4,617 |
| 26230 | 3c | 0,012 | -1,764 | 40,1 | 0,516 | 0,423 | 4,435 |
| 27664 | | 0,011 | -2,549 | 48,1 | 0,435 | 0,331 | 4,293 |
| 1832 | | 0,008 | -2,605 | 37,1 | 1,008 | 0,299 | 3,773 |
| 7592 | | 0,010 | -2,595 | 49,7 | 0,520 | 0,277 | 3,617 |
| 17728 | | 0,010 | -2,627 | 54,4 | 0,714 | 0,340 | 3,571 |
| 7146 | 3d | 0,009 | -2,036 | 35,4 | 1,441 | 0,342 | 3,546 |
| 15805 | | 0,012 | -1,805 | 33,5 | 0,639 | 0,431 | 3,218 |
| 15409 | | 0,013 | -1,830 | 34,1 | 1,169 | 0,468 | 3,169 |
| 14440 | | 0,009 | -2,133 | 27,0 | 1,503 | 0,327 | 2,990 |
| 17650 | | 0,010 | -2,246 | 53,0 | 0,642 | 0,310 | 2,360 |
| 9674 | | 0,008 | -1,957 | 52,7 | 1,017 | 0,265 | 1,925 |
| 30047 | | 0,011 | -1,547 | 44,2 | 0,589 | 0,508 | 1,512 |
| 11346 | | 0,012 | -1,800 | 38,7 | 0,811 | 0,426 | 1,423 |
| 30486 | | 0,011 | -1,959 | 35,9 | 0,670 | 0,563 | 1,256 |
| 8344 | | 0,010 | -1,922 | 32,6 | 2,057 | 1,130 | 1,137 |
| 20277 | | 0,012 | -1,712 | 39,7 | 0,533 | 0,842 | 1,126 |
| 380 | | 0,013 | -1,794 | 48,2 | 0,641 | 0,395 | 1,045 |
| 10474 | | 0,013 | -1,808 | 32,5 | 0,789 | 0,711 | 1,019 |
| 16159 | | 0,013 | -1,314 | 27,4 | 0,513 | 2,275 | 0,892 |
| 15009 | | 0,013 | -1,909 | 34,4 | 0,754 | 0,819 | 0,858 |
| 2630 | | 0,010 | -1,922 | 34,6 | 0,793 | 0,393 | 0,779 |
| 27197 | | 0,012 | -1,468 | 32,1 | 0,840 | 0,673 | 0,775 |
| 13726 | | 0,012 | -1,641 | 38,8 | 1,614 | 0,696 | 0,730 |
| 18746 | | 0,011 | -1,914 | 46,9 | 0,794 | 0,384 | 0,522 |

One can observe that solutions 29884 (Fig. 3a) and 26230 (Fig. 3c) exhibit a low value of criterion c_4 , leading to the displacement of the knee joint E to an undesirable lower position that does not conform to human anatomy. Solution 31076 (Fig. 3b) possesses an acceptable c_4 value, but the straight-line segment height $H = -c_2 = -\eta^0$ is excessive. Same shortcomings take place in solutions 27664, 1832, 7592, and 17728, thus the relevant figures have not been plotted. Ultimately, our analysis identified solution 7146 (Fig. 3d) as the most suitable choice. Although it exhibits a suboptimal swing height, it has excellent accuracy, transmission angle, and a satisfactory knee joint position E . As demonstrated in Fig. 3, the lower the c_6 value, the lower the foot swing height (h). Thus, the rest of the solutions are not shown.

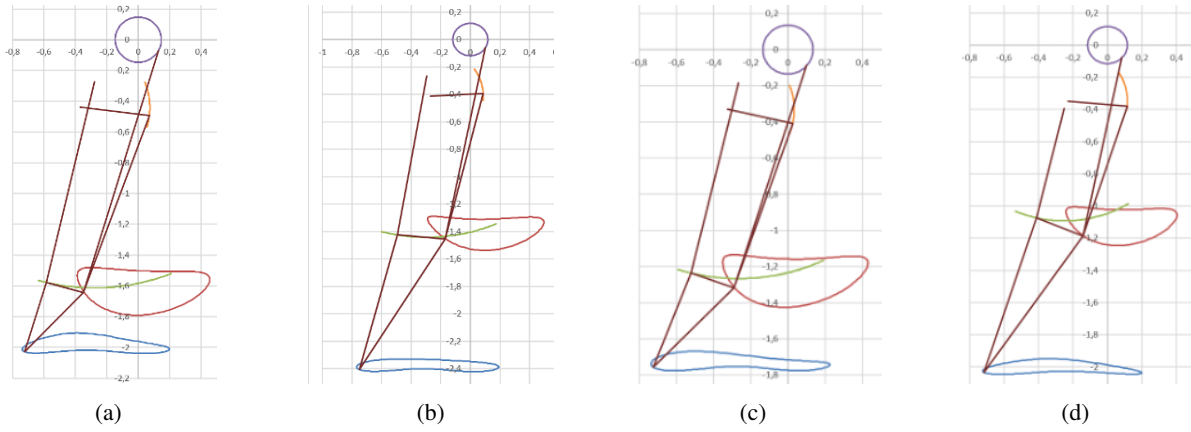


Fig. 3: Visualization of the mechanisms with swing phase trajectories turned inward

Table 3: Solution 7146 design parameters p_1, \dots, p_7

| LP τ N $^{\circ}$ | X_D | Y_D | X_G | Y_G | r_{AB} | φ_0 | Φ |
|---------------------------|----------|----------|----------|----------|----------|-------------|-----------|
| 7146 | -0,22953 | -0,34842 | -0,25044 | -0,39308 | 0,11482 | -43,16928 | 185,16479 |

Table 4: Solution 7146 design parameters p_8, \dots, p_{13}

| LP τ N $^{\circ}$ | L_{BC} | L_{CD} | x_E | y_E | L_{EF} | L_{FG} |
|------------------------|----------|----------|---------|----------|----------|----------|
| 7146 | 0.30241 | 0.34472 | 1.08084 | -0.33612 | 0.29188 | 0.69900 |

Table 5: Solution 7146 design parameters parameters x_1, x_2, \dots, x_5

| LP τ N $^{\circ}$ | x_1 | x_2 | x_3 | x_4 | x_5 |
|------------------------|---------|---------|----------|----------|---------|
| 7146 | 0.19607 | 1.00248 | -0.71623 | -2.03609 | 0.90610 |

6 Local Search and Final Mechanism Design

In order to improve the swing height the local search around the solution 7146 is carried out. The selected solutions presented on Table 6, arranged in descending order of the criterion c_6 .

Because of the substantial number of solutions, we included only few images on Fig. 4, Table 7 explains why we have selected these specific images. The remaining solutions are not depicted, since one can observe, that step height decreases. The design parameters for the solution 8398 are presented on Tables 8 – 10.

Table 6: The results of the local search around the solution 7146: the best solutions by criterion c_6

| LPτ № | Fig. | c_1 | c_2 | c_3 | c_4 | c_5 | c_6 |
|-------|------|---------------|---------------|-------------|-------|-------|--------------|
| 5380 | 4a | 0.010 | -2.288 | 20.6 | 1.199 | 0.347 | 9.385 |
| 20757 | | 0.011 | -2.101 | 22.2 | 1.278 | 0.389 | 8.880 |
| 16365 | | 0.011 | -2.112 | 23.6 | 1.100 | 0.373 | 8.817 |
| 22170 | | 0.011 | -2.156 | 22.1 | 1.427 | 0.351 | 8.361 |
| 17370 | 4b | 0.010 | -2.176 | 23.7 | 1.220 | 0.346 | 8.337 |
| 29005 | 4c | 0.011 | -2.096 | 25.3 | 1.228 | 0.372 | 8.242 |
| 19111 | | 0.011 | -2.031 | 22.0 | 1.317 | 0.390 | 8.161 |
| 26668 | | 0.010 | -2.223 | 24.3 | 1.210 | 0.367 | 8.070 |
| 13257 | | 0.011 | -2.110 | 23.3 | 1.415 | 0.331 | 8.060 |
| 17228 | | 0.011 | -2.201 | 22.1 | 1.502 | 0.334 | 8.053 |
| 17743 | | 0.012 | -1.972 | 20.2 | 1.409 | 0.368 | 8.052 |
| 19215 | | 0.012 | -1.992 | 22.1 | 1.327 | 0.383 | 7.986 |
| 8398 | 4d | 0.011 | -2.171 | 26.9 | 1.260 | 0.376 | 7.934 |
| 3766 | | 0.010 | -2.173 | 23.7 | 1.342 | 0.343 | 7.924 |
| 23411 | | 0.012 | -2.066 | 27.1 | 1.331 | 0.377 | 7.920 |
| 30022 | | 0.011 | -2.158 | 24.6 | 1.278 | 0.418 | 7.913 |
| 12749 | | 0.011 | -2.096 | 26.2 | 1.358 | 0.347 | 7.861 |
| 30915 | | 0.011 | -2.033 | 22.2 | 1.276 | 0.384 | 7.769 |
| 1031 | | 0.011 | -2.071 | 28.4 | 1.230 | 0.389 | 7.749 |
| 3628 | | 0.011 | -2.215 | 25.9 | 1.235 | 0.402 | 7.727 |
| 3327 | | 0.012 | -1.985 | 22.3 | 1.224 | 0.428 | 7.704 |
| 10981 | | 0.011 | -2.078 | 23.0 | 1.310 | 0.395 | 7.680 |
| 10134 | | 0.010 | -2.165 | 24.6 | 1.171 | 0.364 | 7.665 |
| 4693 | | 0.011 | -2.077 | 22.4 | 1.165 | 0.422 | 7.663 |
| 2872 | 4e | 0.0098 | -2.227 | 24.1 | 1.466 | 0.312 | 7.630 |
| 20824 | | 0.011 | -2.282 | 23.4 | 1.044 | 0.364 | 7.619 |
| 31 | | 0.010 | -2.030 | 22.7 | 1.090 | 0.374 | 7.618 |
| 15153 | | 0.010 | -2.111 | 23.0 | 1.335 | 0.384 | 7.617 |
| 28345 | 4f | 0.011 | -2.138 | 29.2 | 1.255 | 0.363 | 7.603 |

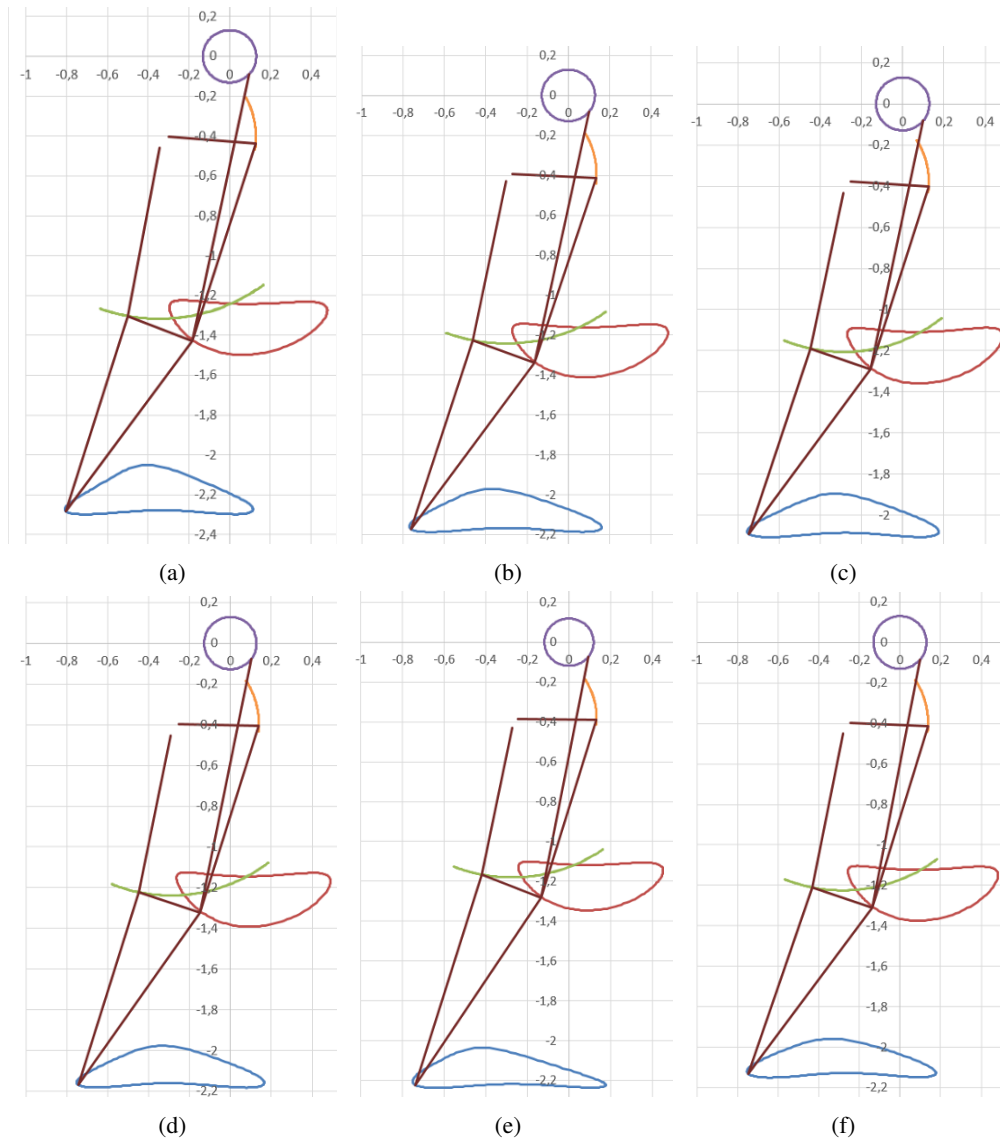


Fig. 4: The results by the local search with improved swing height

Table 7: Comments to the images

| LPτ № | Fig. | Comments |
|-------|------|---|
| 5380 | 4a | The best solution by swing height, the accuracy is high |
| 17370 | 4b | The best solution by the accuracy, step height is high |
| 29005 | 4c | Transmission angle and height H are better than in previous solutions, swing height and the accuracy are high as well |
| 8398 | 4d | Trying to improve transmission angle we come to this solution |
| 2872 | 4e | The best accuracy 0.0098 |
| 28345 | 4f | The best transmission angle 29.2 |

Table 8: Design parameters p_1, \dots, p_7 for solution 8398

| LPτ № | X_D | Y_D | X_G | Y_G | r_{AB} | φ_o | ■ |
|-------|----------|----------|----------|----------|----------|-------------|----------|
| 8398 | -0.25122 | -0.39679 | -0.29140 | -0.45175 | 0.12829 | -37.87341 | 183.5455 |

Table 9: Design parameters p_8, \dots, p_{13} for solution 8398

| LPτ № | L_{BC} | L_{CD} | x_E | y_E | L_{EF} | L_{FG} |
|-------|----------|----------|---------|----------|----------|----------|
| 8398 | 0.32738 | 0.39084 | 1.20469 | -0.39171 | 0.31884 | 0.78648 |

Table 10: Design parameters x_1, x_2, \dots, x_5 for solution 8398

| LPτ № | x_1 | x_2 | x_3 | x_4 | x_5 |
|-------|---------|---------|----------|----------|---------|
| 8398 | 0.30476 | 0.99082 | -0.74396 | -2.17071 | 0.90412 |

7 Conclusions

The typical schemes of leg exoskeletons are based on open-loop kinematic chain with the motors mounted directly on the moveable joints. While the design choice offer greater flexibility and ease of design, their large number of DOF contributes to increased costs and complexities in control. Using heavy servo-motors to meet significant torques aroused in active joints leads to complicated and cumbersome design. Existing literature emphasizes bulkiness and substantial weight of this kind of devices.

Another approach involves the utilization of 1-DOF mechanisms. However, many of them characterized by a substantial number of linkages, often reaching eight or more. For example, the best schemes of such design are selected in figure below. As you can see in Fig. 5, even the mechanism (b), which is often considered the best and published in the MMT International Journal as one of the respectable designs [28], is overly bulky with a large number of links also. If employed as an lower-limb exoskeleton mechanism, its geometry would not align with the human anatomy. In the figure also shown that the mechanism we designed (a) is well-suited to the anatomical parameters of humans. Note, that the numbers on the axes are relative values (not in meters), when L — the step length — is equal to 1.

In this study, we introduced a novel synthesis method with analytical solutions provided for synthesizing lower-limb exoskeleton. Additionally, we have incorporated multicriteria optimization by six designing criteria. As a result, we offer several mechanisms, comprising only six links, well-suited to the human anatomical structure, exhibit superior trajectory accuracy, efficient force transmission, satisfactory step height, and having internal transfer segment of the foot.

Acknowledgements

This work was supported by the Science Committee of the Ministry of Education and Science of the Republic of Kazakhstan under Grant AP14870080 "Structural-Parametric Synthesis of the Musculoskeletal Mechanisms of the Exoskeleton of the lower limb". The authors would like to express their gratitude King Abdullah University of Science and Technology for their partial financial support.

References

- [1] Mikolajczyk, Tadeusz, Emilia Mikołajewska, Hayder FN Al-Shuka, Tomasz Malinowski, Adam Kłodowski, Danil Yurievich Pimenov, Tomasz Paczkowski, Fuwen Hu, Khaled Giasin, Dariusz Mikołajewski, et al. 2022. "Recent Advances in Bipedal Walking Robots: Review of Gait, Drive, Sensors and Control Systems." *Sensors* 22 (12): 4440. MDPI.
- [2] Shi, Di, Wuxiang Zhang, Wei Zhang, and Xilun Ding. 2019. "A Review on Lower Limb Rehabilitation Exoskeleton Robots." *Chinese Journal of Mechanical Engineering* 32 (1): 1–11. Springer.

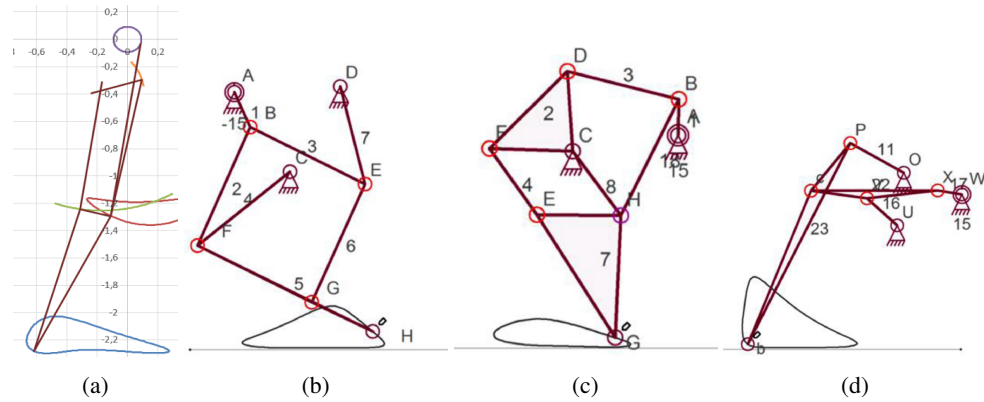


Fig. 5: a) Our 6-bar mechanism; b) 8-bar Peaucellier-Lipkin type mechanism [28]; c) Theo Jansen's Linkage [28]; d) Joseph Klann's Linkage [28]

- [3] Tijjani, Ibrahim, Shivesh Kumar, and Melya Boukheddimi. 2022. "A Survey on Design and Control of Lower Extremity Exoskeletons for Bipedal Walking." *Applied Sciences* 12 (5): 2395. MDPI.
- [4] Sanchez-Villamañan, Maria del Carmen, Jose Gonzalez-Vargas, Diego Torricelli, Juan C Moreno, and Jose L Pons. 2019. "Compliant Lower Limb Exoskeletons: A Comprehensive Review on Mechanical Design Principles." *Journal of Neuroengineering and Rehabilitation* 16 (1): 1–16. BioMed Central.
- [5] Copilusi, Cristian, Sorin Dumitru, Ionut Geonea, Leonard Gherge Ciurezu, and Nicolae Dumitru. 2022. "Design Approaches of an Exoskeleton for Human Neuromotor Rehabilitation." *Applied Sciences* 12 (8): 3952. MDPI.
- [6] Shen, Zefang, Tele Tan, Garry Allison, and Lei Cui. 2019. "A Customized One-Degree-of-Freedom Linkage Based Leg Exoskeleton for Continuous Passive Motion Rehabilitation." In *Advances in Italian Mechanism Science: Proceedings of the Second International Conference of IFToMM Italy*, 518–526. Springer.
- [7] Shen, Zefang, Garry Allison, and Lei Cui. 2018. "An Integrated Type and Dimensional Synthesis Method to Design One Degree-of-Freedom Planar Linkages with Only Revolute Joints for Exoskeletons." *Journal of Mechanical Design* 140 (9): 092302. American Society of Mechanical Engineers.
- [8] Terefe, Tesfaye Olana, and Hirpa G Lemu. 2019. "Review and Synthesis of a Walking Machine (Robot) Leg Mechanism." EDP Sciences.
- [9] Liu, JH, B Li, Q Ning, M Zhou, YX Li, MC Liu, and K Xu. 2022. "Mechanical Design of a Passive Lower-Limb Exoskeleton for Load-Carrying Assistance." In *Journal of Physics: Conference Series*, 2213 (1): 012035. IOP Publishing.
- [10] Geonea, I, D Tarnita, Giuseppe Carbone, and M Ceccarelli. 2019. "Design and Simulation of a Leg Exoskeleton Linkage for Human Motion Assistance." In *New Trends in Medical and Service Robotics: Advances in Theory and Practice*, 93–100. Springer.
- [11] Tarnita, D, I Geonea, A Petcu, and DN Tarnita. 2018. "Numerical Simulations and Experimental Human Gait Analysis Using Wearable Sensors." In *New Trends in Medical and Service Robots: Design, Analysis and Control* 5, 289–304. Springer.
- [12] Geonea, Ionut, Nicolae Dumitru, Daniela Tarnita, and Paul Rinderu. 2019. "Design and Kinematics of a New Leg Exoskeleton for Human Motion Assistance." In *Advances in Mechanism and Machine Science: Proceedings of the 15th IFToMM World Congress on Mechanism and Machine Science* 15, 165–174. Springer.
- [13] Al-Araidah, O, W Batayneh, T Darabseh, and SM BaniHani. 2011. "Conceptual Design of a Single DOF Human-Like Eight-Bar Leg Mechanism." *JJMIE* 5 (4).
- [14] Batayneh, Wafa, Omar Al-Araidah, and Salaheddin Malkawi. 2013. "Biomimetic Design of a Single DOF Stephenson III Leg Mechanism." *Mechanical Engineering Research* 3 (2): 43. Canadian Center of Science and Education.
- [15] Brown, Brett C. 2006. "Design of a Single-Degree-of-Freedom Biped Walking Mechanism." PhD thesis, The Ohio State University.
- [16] Giesbrecht, Daniel. 2010. "Design and Optimization of a One-DOF Eight-Bar Leg Mechanism for a Walking Machine." Master's thesis, The University of Manitoba, Winnipeg, Manitoba. 95.
- [17] Punde, Yash, Yugandhar Dhande, and Amit Chopde. 2020. "Design and Linkage Analysis of Theo Jansen Mechanism." *International Journal of Engineering Research and Technology* 9 (09): 259–263. IJERT.
- [18] Pop, F, E-Ch Lovasz, C Pop, and V Dolga. 2016. "Dimensional Synthesis of a Leg Mechanism." In *IOP Conference Series: Materials Science and Engineering*, 147 (1): 012083. IOP Publishing.
- [19] Kulandaidsaan Sheba, Jaichandar, Mohan Rajesh Elara, Edgar Martínez-García, and Le Tan-Phuc. 2016. "Trajectory Generation and Stability Analysis for Reconfigurable Klann Mechanism Based Walking Robot." *Robotics* 5 (3): 13. MDPI.

- [20] Lokhande, NG, and VB Emche. 2013. “Mechanical Spider by Using Klann Mechanism.” *International Journal of Mechanical Engineering and Computer Applications* 1 (5): 13–16.
- [21] Soyguder, Servet, and Hasan Alli. 2007. “Design and Prototype of a Six-Legged Walking Insect Robot.” *Industrial Robot: An International Journal* 34 (5): 412–422. Emerald Group Publishing Limited.
- [22] Komoda, Kazuma, and Hiroaki Wagatsuma. 2012. “A Proposal of the Extended Mechanism for Theo Jansen Linkage to Modify the Walking Elliptic Orbit and a Study of Cyclic Base Function.” In *Proceedings of the 7th Annual Dynamic Walking Conference (DWC’12)*.
- [23] Tsuge, Brandon Yukio. 2015. “Kinematics Synthesis of Lower Limb Supporting Linkages.” University of California, Irvine.
- [24] Ferreira, João P., Manuel M. Crisostomo, and A. Paulo Coimbra. 2009. “Human Gait Acquisition and Characterization.” *IEEE Transactions on Instrumentation and Measurement* 58 (9): 2979–2988. doi:10.1109/TIM.2009.2016801.
- [25] Ishmael, Marshall K, Dante Archangeli, and Tommaso Lenzi. 2022. “A Powered Hip Exoskeleton with High Torque Density for Walking, Running, and Stair Ascent.” *IEEE/ASME Transactions on Mechatronics* 27 (6): 4561–4572. IEEE.
- [26] Plecnik, M, and JM McCarthy. 2013. “Dimensional Synthesis of Six-Bar Linkage as a Constrained RPR Chain.” In *New Trends in Mechanism and Machine Science: Theory and Applications in Engineering*, 273–280. Springer.
- [27] Plecnik, Mark M, and J Michael McCarthy. 2016. “Design of Stephenson Linkages that Guide a Point Along a Specified Trajectory.” *Mechanism and Machine Theory* 96: 38–51. Elsevier.
- [28] Desai, Shivamanappa G, Anandkumar R Annigeri, and A TimmanaGouda. 2019. “Analysis of a New Single Degree-of-Freedom Eight Link Leg Mechanism for Walking Machine.” *Mechanism and Machine Theory* 140: 747–764. Elsevier.
- [29] Kim, Hyun-Gyu, Min-Suck Jung, Jae-Kyun Shin, and TaeWon Seo. 2014. “Optimal Design of Klann-Linkage Based Walking Mechanism for Amphibious Locomotion on Water and Ground.” *Journal of Institute of Control, Robotics and Systems* 20 (9): 936–941. Institute of Control, Robotics and Systems.
- [30] Komoda, Kazuma, and Hiroaki Wagatsuma. 2017. “Energy-Efficacy Comparisons and Multibody Dynamics Analyses of Legged Robots with Different Closed-Loop Mechanisms.” *Multibody System Dynamics* 40: 123–153. Springer.
- [31] Xu, Ke, Haitao Liu, Xingqiao Zhu, and Yongbin Song. 2019. “Kinematic Analysis of a Novel Planar Six-Bar Bionic Leg.” In *Advances in Mechanism and Machine Science: Proceedings of the 15th IFToMM World Congress on Mechanism and Machine Science 15*, 13–21. Springer.
- [32] Roman Statnikov. 1999. *Multicriteria Design: Optimization and Identification*. Vol. 26. Springer Science & Business Media.
- [33] Ibrayev, Sayat M, and Nutpulla K Jamalov. 2002. “Approximate Synthesis of Planar Cartesian Manipulators with Parallel Structures.” *Mechanism and Machine Theory* 37 (9): 877–894. Elsevier.
- [34] Ibrayev, S.M. 2014. *Approximate Synthesis of Planar Linkages: Methods and Numerical Analysis*. Almaty, 356 pages. (in Russian)
- [35] Ibrayev, Sayat, Arman Ibrayeva, Nutpulla Jamalov, and Sarosh H Patel. 2022. “Optimization of the Walking Robot Parameters on the Basis of Isotropy Criteria.” *IEEE Access* 10: 113969–113979. IEEE.
- [36] Ibrayev, Sayat, Nutpulla Jamalov, Arman Ibrayeva, and Gaukhar Mukhambetkaliyeva. 2019. “Optimal Structural Synthesis of Agricultural Legged Robot with Minimal Damage on Soil.” In *E3S Web of Conferences*, 135: 01027. EDP Sciences.
- [37] Ibrayev, Sayat, Arman Ibrayeva, Nutpulla Jamalov, Aidos Ibrayev, Zhomart Ualiyev, and Bekzat Amanov. 2023. “Optimal Synthesis of Walking Robot Leg.” *Mechanics Based Design of Structures and Machines*, 1–21. Taylor & Francis.
- [38] Ibrayev, Sayat, Nutpulla Jamalov, Amandyk Tuleshov, Assylbek Jomartov, Aidos Ibrayev, Aziz Kamal, Arman Ibrayeva, and Kuatbay Bissembayev. 2020. “Walking Robot Leg Design Based on Translatory Straight-Line Generator.” In *Symposium on Robot Design, Dynamics and Control*, 264–271. Springer.

Appendix A: Kinematics of the Lower Limb Exoskeleton Mechanism

The absolute coordinates of joints B and C are simply determined as follows:

$$\begin{aligned}\xi_B &= \xi_A + r_{AB} \cos \varphi \\ \eta_B &= \eta_A + r_{AB} \sin \varphi\end{aligned}\quad (43)$$

$$\begin{aligned}\xi_C &= \xi_B + l_{BC} \cos \varphi_{BC} \\ \eta_C &= \eta_B + l_{BC} \sin \varphi_{BC},\end{aligned}\quad (44)$$

where the angular position $\varphi_{BC} = \angle(\vec{A\xi}, \vec{B\xi})$ (Fig. 6) of link BC is defined as

$$\varphi_{BC} = \alpha_{BD} + \alpha_{DBC}, \quad (45)$$

$$\alpha_{BD} = \angle(\vec{A\xi}, \vec{BD}) = \text{atan2}(\xi_D - \xi_B, \eta_D - \eta_B), \quad (46)$$

$$\alpha_{DBC} = \arccos \frac{|BD|^2 + l_{BC}^2 - l_{CD}^2}{2l_{BC}|BD|}, \quad (47)$$

$$|BD|^2 = (\xi_D - \xi_B)^2 + (\eta_D - \eta_B)^2. \quad (48)$$

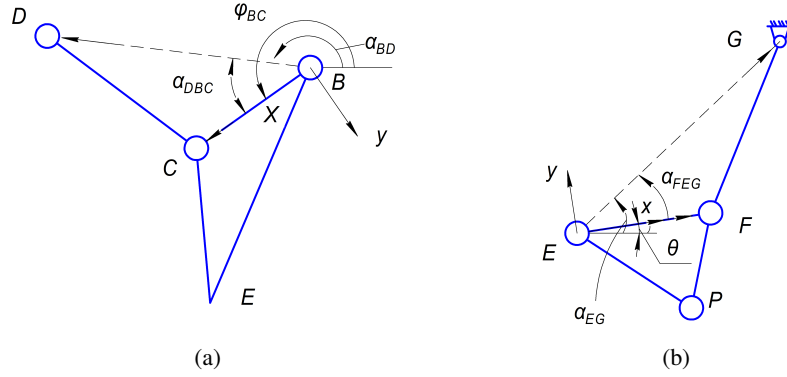


Fig. 6: Kinematic scheme of a lower-limb exoskeleton mechanism

The absolute coordinates of the joint E are

$$\begin{aligned} \xi_E &= \xi_B + x_E \cos \varphi_{BC} - y_E \sin \varphi_{BC} \\ \eta_E &= \eta_B + x_E \sin \varphi_{BC} + y_E \cos \varphi_{BC}, \end{aligned} \quad (49)$$

where x_E, y_E are local coordinates of joint E relative to Bxy . Now, in the same way we analyse the dyad EF , and determine the absolute coordinates of joint F :

$$\begin{aligned} \xi_F &= \xi_E + l_{EF} \cos \varphi_{EF} \\ \eta_F &= \eta_E + l_{EF} \sin \varphi_{EF}, \end{aligned} \quad (50)$$

where $\varphi_{EF} = \angle(\vec{A\xi}, \vec{EF})$ is determined as:

$$\varphi_{EF} = \alpha_{EG} + \alpha_{FEG} \quad (51)$$

$$\alpha_{EG} = \angle(\overrightarrow{A\xi}, \overrightarrow{EG}) = \text{atan2}(\xi_G - \xi_E, \eta_G - \eta_E) \quad (52)$$

$$\alpha_{FEG} = \arccos \frac{|EG|^2 + l_{EF}^2 - l_{FG}^2}{2l_{EF}|EG|} \quad (53)$$

$$|EG|^2 = (\xi_G - \xi_E)^2 + (\eta_G - \eta_E)^2. \quad (54)$$

The equations for the foot-center P are given in the Section 2.

Appendix B: Proof of the Optimization Condition

The original $2N$ constraint equations ($\delta_i^\xi = 0, \delta_i^\eta = 0$) can be written in the form:

$$\begin{aligned} \delta_i^\xi = 0: \quad & \cos \theta_i x_1 - \sin \theta_i x_2 - x_3 - \frac{i-1}{N-1} x_5 + \xi_{E_i} = 0, \quad i = \overline{1, N} \\ \delta_i^\eta = 0: \quad & \sin \theta_i x_1 + \cos \theta_i x_2 - x_4 - \eta_{E_i} = 0. \end{aligned} \quad (55)$$

Let us write these equations in the matrix form:

$$[\Gamma_i \mid -T_i] \vec{x} = \begin{bmatrix} -\xi_{E_i} \\ -\eta_{E_i} \end{bmatrix}, \quad (56)$$

where

$$\Gamma_i = \begin{bmatrix} \cos \theta_i & -\sin \theta_i \\ \sin \theta_i & \cos \theta_i \end{bmatrix}, \quad (57)$$

$$T_i = \begin{bmatrix} 1 & 0 & \frac{i-1}{N-1} \\ 0 & 1 & 0 \end{bmatrix}, \quad (58)$$

$$\dim \Gamma_i = 2 \times 2, \quad \dim T_i = 2 \times 3. \quad (59)$$

Then the linear system of equations (5×5) for determining \vec{x} can be written in the form

$$H_1^T H_1 \vec{x} = H_1^T \vec{c}_1, \quad (60)$$

where H_1 is the matrix of dimension $\dim H_1 = 2N \times 5, \dim \vec{c}_1 = 2N$:

$$H_1 = \begin{bmatrix} \Gamma_1 & -T_1 \\ \Gamma_2 & -T_2 \\ \vdots & \vdots \\ \Gamma_N & -T_N \end{bmatrix} \quad (61)$$

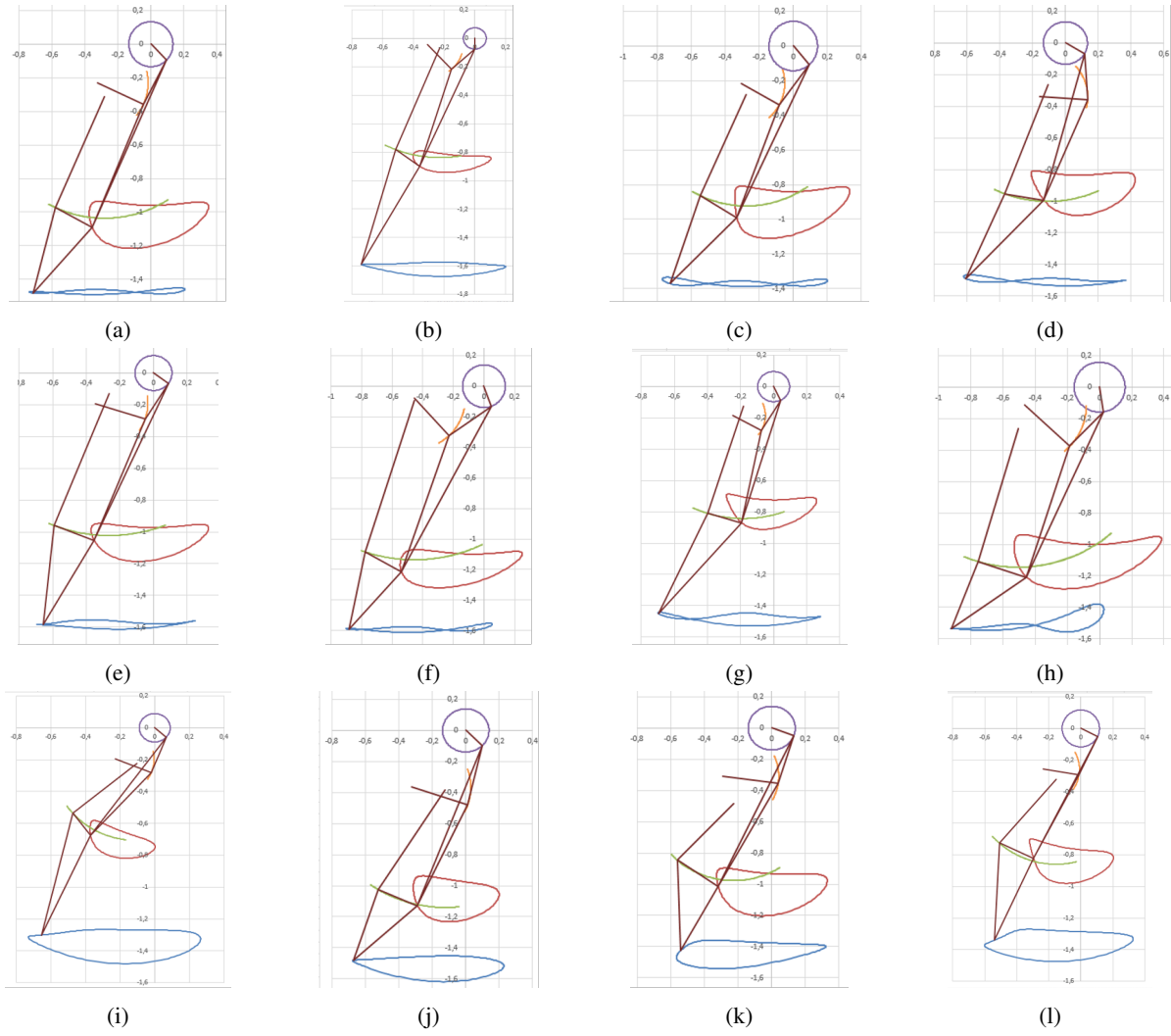


Fig. 7: Functionality study of 6 bar mechanism

$$c_1 = \begin{bmatrix} \xi_{E_1} \\ \eta_{E_1} \\ \xi_{E_2} \\ \eta_{E_2} \\ \vdots \\ \xi_{E_N} \\ \eta_{E_N} \end{bmatrix} \quad (62)$$

Thus, the Hessian matrix H_S will be

$$\frac{d^2S}{d\bar{x}^2} = H_1^T H_1 \quad (63)$$

Therefore, the matrix H_S is non-negative definite, $\det H_S = 0$ is the singularity of the synthesis problem.

Appendix C

Table 11: Random search design parameters p_1, \dots, p_7 for the mechanism on Fig. 7a

| LPτ № | ξ_D | η_D | ξ_G | η_G | r_{AB} | φ_0 | Φ |
|-------|----------|----------|----------|----------|----------|-------------|-----------|
| 19597 | -0,32133 | -0,23007 | -0,28094 | -0,31117 | 0,13375 | -45,44359 | 183,12408 |

Table 12: Random search design parameter values p_8, \dots, p_{13} for the mechanism on the Fig. 7a

| LPτ № | L_{BC} | L_{CD} | x_E | y_E | L_{EF} | L_{FG} |
|-------|----------|----------|---------|---------|----------|----------|
| 19597 | 0.29670 | 0.30422 | 1.09131 | 0.06663 | 0.25049 | 0.72561 |

Table 13: The parameters x_1, x_2, \dots, x_5 for the mechanism on the Fig. 7a

| LPτ № | Fig | x_1 | x_2 | x_3 | x_4 | x_5 |
|-------|-----|---------|---------|----------|----------|---------|
| 19597 | 7a | 0.12676 | 0.51165 | -0.71130 | -1.47377 | 0.91107 |